

THE EFFECT OF ADDING SILICON AND ZINC ELEMENTS ON THE MECHANICAL PROPERTIES OF CLOSED-CELL ALUMINUM-BASED FOAMS

M. R. Farahani, H. R. Rezaei Ashtiani and S. H. Elahi

Department of Mechanical Engineering, Arak University of Technology, Arak 38135-1177, Iran

Copyright © 2022 American Foundry Society
<https://doi.org/10.1007/s40962-022-00827-4>

Abstract

The melt-foaming method is a commercial process to produce metallic foams. In the present research, closed-cell aluminum foams with different silicon and zinc contents (4%Si-4%Zn, 4%Si-8%Zn, 8%Si-4%Zn, 8%Si-8%Zn) using the calcium as a viscosity enhancer and calcium carbonate (CaCO_3) as a foaming agent by the melt-foaming method was successfully prepared. The compression test was used to determine the effects of the combination of silicon and zinc elements on the compressive behavior of fabricated foams. According to the x-ray diffraction analysis, the SiO_2 , CaAl_2Si_2 , $\text{Ca}_{14}\text{Al}_{10}\text{Zn}_6\text{O}_{35}$, and $\text{Ca}_3\text{Al}_{14}\text{ZnO}_{10}$ phases have been created by adding silicon and zinc elements in samples. Phases and intermetallic compounds

created in the cell walls of Al-4%Si-4%Zn and Al-4%Si-8%Zn samples have a uniform distribution which increased the strength and energy absorption of these foams. The results show that the CaAl_2Si_2 brittle phase is present in the structure of Al-8%Si-4%Zn and Al-8%Si-8%Zn samples also, the formation of the needle-shaped structures and intermetallic compounds has reduced the strength of these foams.

Keywords: aluminum foam, silicon, zinc, energy absorption, compressive property

Introduction

The design and construction of lightweight structures with high strength have been considered in recent years. In this regard, researchers are constantly trying to replace materials with proper strength and stiffness for a variety of applications and reduce energy consumption at the same time.¹⁻³ Metal foam is one of these materials that has attracted the attention of researchers and craftsmen.⁴ The main reason for the tendency toward metal foams is the proper strength-to-weight ratio of this material in comparison with the same volume of metal.⁵ Besides, metal foams have high energy absorption properties.^{6,7} Today, these materials have been widely used in various fields of industry and research, including medical implants, filters, and buffers.⁸⁻¹⁰ It can be said that the highest use of these materials in the industry is due to their high strength-to-weight ratio and high energy absorption capacity which leads to the use of these materials in the automotive and aerospace industries.^{8,11} There are many methods to manufacture metal foams¹² but among these methods, melt-

foaming and powder metallurgy methods have been considered more than the other methods.^{5,13-17} It has been reported that the mechanical properties of the foam are dependent on the mechanical properties of the base material. In this regard, many efforts have been made to improve the compressive properties and increase the strength of foams with low-cost methods such as heat treatment^{18,19} using high-strength aluminum alloy,²⁰ and alloying.²¹⁻²³ Xia et al.²⁴ studied the effect of Mn elements on the compressive and mechanical properties of the aluminum foam and the results showed that the distribution of manganese elements in the forms of MnO_2 , Al_6Mn intermetallic phase, Al-Mn solid solution, and undissolved Mn particles in the cell wall structure of these foams was formed. Also, results showed that Mn improved the microhardness, plateau region, and yield strength of the metal foam. The effects of the addition and distribution of erbium elements on the structure and mechanical properties of closed-cell aluminum foams were investigated by Zhao et al.²⁵ The results of their research showed that erbium significantly improves the dendritic structure of aluminum foam; also increases the strength, energy absorption, and microhardness of the cell wall of Er-containing foams compared to the commercial pure aluminum foam, however, the

mechanical efficiency of the foam is reduced by an additional amount of erbium of more than 0.5 wt%. In a study on the effect of silicon content on mechanical properties of aluminum-zinc-silicon alloys, it was observed that the microstructure of the aluminum-zinc-silicon alloys consisted of rich aluminum and zinc phases and silicon particles, which were found to be the size and distribution of the silicon particles depend on the silicon content of these alloys.²⁶ Also, the investigations show that silicon addition has a significant effect on mechanical and wear resistance properties of zinc-based alloys and the density of alloys decreases with increasing silicon contents. The hardness and the tensile strength of the alloys increased with increasing silicon content up to 2 wt%, whereas they decreased for above this amount (2 wt%). However, the elongation percentage of these alloys decreased with increasing silicon content up to 3 wt%, whereas the elongation increased with increasing the silicon content above this amount (3 wt%).²⁶ Soo-Han Park et al. investigated the effects of Si, Cu, and Zn additions on the pure aluminum melt, they observed that the surface tension decreases and the viscosity of the melt increases with the addition of Si, Cu, and Zn to the melt.²⁷ The results of our previous work on the effect of zinc content on the mechanical properties of closed-cell aluminum foams showed that the addition of zinc with various percentages; causes an increase in viscosity, density, and cell wall thickness, and also the formation of the oxide phases in these foams.²⁸ Also in previous research, the effect of silicon addition with various percentages was investigated on the mechanical properties of closed-cell aluminum foams, and the results showed that the addition of silicon increases the viscosity and decreases the surface tension of the melt. The cell size increases and cell wall thickness decreases with increasing the amount of Si from 4 to 8 wt%, also the CaAl₂Si₂ brittle phase was formed in the sample with 8%Si and the strength of this sample compare to the other samples was reduced.²⁹

The effect of each of the silicon and zinc elements was alone studied in a small number of researches and the combined effect of these elements with different percentages has not been investigated. According to the results of previous experiments on foams containing silicon and zinc (Al-Si and Al-Zn), it was found that the aluminum alloy foams with 4 to 8wt% of silicon and zinc elements have better mechanical properties than other percentages of silicon and zinc elements; so in this study, the effect of combining these elements with different weight percentages (4 to 8wt%) have been investigated on the physical and mechanical properties of closed-cell aluminum foams.

Experimental Approach

Sample Preparation

In this study, the AA1080 aluminum ingot was used as a base metal and calcium granule and CaCO₃ were used as a

Table 1. Chemical Composition of Pure Aluminum (AA1080)

Element	Al	Fe	Si	Ga	V
Wight%	99.8%	0.07	0.04%	0.01%	0.01%

thickening and foaming agent, respectively, moreover, zinc and silicon particles as the additive materials were used for alloying. The chemical composition of the base material is shown in Table 1. The preparation steps of the desired alloy foams are as follows:

At first, about 1kg of pure aluminum was melted in a graphite crucible at a constant temperature of 800 °C. An electric resistance furnace was used for melting aluminum and foaming preparation. Then to make each sample, a certain quantity of silicon and zinc with the different contents of (4%Si-4%Zn, 4%Si-8%Zn, 8%Si-4%Zn, and 8%Si-8%Zn, hereinafter refers to as wt%) were added to the melt and they were stirred at the stirring speed of 1200 rpm for 10 min until all of the silicon and zinc particles were uniformly distributed into the melted aluminum. After the silicon and zinc were completely distributed into the melt, calcium (1.5 wt%) was added to the melt and the melt was stirred with a stirring speed of 1200 rpm for 10 min to achieve a suitable viscosity. Then, the melt was poured into the preheated steel mold and CaCO₃ as a foaming agent to a rate of 1.5 wt% was added, and the melt to achieve a uniform distribution of CaCO₃ was stirred with a stirring speed of 1200 rpm for 6 min. The melt was held at the temperature of 700–750 °C to allow the blowing agent was completely decomposed and the foaming process was completed. Finally, after the foam was formed the steel mold was out from the furnace and it was cooled in the air. The mentioned conditions are the same for the whole foaming process except for silicon and zinc contents.

The density and porosity of all samples are calculated using Eqns. 1 and 2:

$$\rho = \frac{M}{V} \quad \text{Eqn. 1}$$

$$\varphi = \frac{(\rho_s - \rho)}{\rho_s} * 100 \quad \text{Eqn. 2}$$

where V is the volume of sample (cm³), M and ρ are the weight (g) and density (gr/cm³) of the sample, respectively, ρ_s is the density of base material and φ is the porosity of samples.^{25,30}

Structure and Microstructure Observation

For microstructural investigations, firstly, the cross-sections of all of the specimens were machined by electro-discharge machining and the specimens were polished, then all of the samples were etched with Keller reagent and

the microstructure of the samples by optical microscopy (OM)(OLYMPUS, DP73) was observed. Then for examining the properties and cell structure the cross section of foams was taken in a photo and the mean cell size of the foams by image J analysis software was obtained. X-ray diffraction analysis was used to detect phase composition by the proper device (X'Pert Pro, Netherland) with CuK α radiation.

Mechanical Properties

Compressive behavior and energy absorption of metallic foams were determined using the compression test at room temperature with a constant cross-head speed of 1 mm/min according to ISO 13314 standard for porous materials. All of the samples for the compressive test were cut by an electro-discharging machine into the size (length \times width \times height) of 30 \times 30 \times 30 mm³.³¹ Vaseline was used to minimize friction between samples and pressure plates. The engineering stress–strain curves of the foams according to the results of compressive test data were obtained. The engineering stress of applied load on the main cross-sectional area of samples and engineering strain as the ratio of reduction in length to the original length in compression test was determined. In general, the stress–strain curves for all metal foams are similar and have three distinct sections that are as follows:

- I. The initial region is a linear elastic region and the yield point is located at the end of the area.
- II. Plateau deformation region which the stress slowly increases with the plastic deformation and collapse of cells in compression.
- III. Densification region where stress is sharply increased, while the strain slightly changes.

These regions have been reported by other researchers.^{18,32,33} Metal foams have good energy absorption properties and this characterization causes this group of materials suitable for energy absorbers. The energy absorption capacity of aluminum foams is calculated according to Eqn. 3.^{18,34}

$$W = \int_0^{\varepsilon} \sigma d\varepsilon \quad \text{Eqn. 3}$$

W is the energy absorption capacity, σ is the flow stress and ε is the strain.

Results and Discussion

Structures and Microstructure of Combination Foams

Figure 1 shows the structures of aluminum foam without adding any alloying elements (pure aluminum foam (0%Si-

0%Zn)) and Al-8%Si-8%Zn foam and binary images of these two foams by Image J software.

The physical properties of the foams with different percentages of silicon and zinc elements have been listed in Table 2.

The pore structures of the foams with different percentages of silicon and zinc consisting of 4%Si-4%Zn, 4%Si-8%Zn, 8%Si-4%Zn, and 8%Si-8%Zn are shown in Figure 2(a) to (d), respectively. In previous works^{28,29} on Al-Si and Al-Zn aluminum alloy foams, it was observed that the average cell size in aluminum alloy foam with 4%Si and 4%Zn is smaller than all of the other alloy foam samples, which this item was also observed in this experiment for Al-4%Si-4%Zn foam sample. As is shown in Figure 3 and also the measured results have been obtained from the cell size of the foams by Image J software, the results show that the Al-4%Si-4%Zn foam has the smallest cell size and thickest cell wall; but for Al-4%Si-8%Zn foam, the cell size is slightly larger than the foam with 4%Si-4%Zn it seems that this due to the increasing amount of zinc in this sample which this item was also observed in Al-Zn foam sample containing 8%Zn. As shown in Figure 2, the cell size in Al-8%Si-4%Zn and Al-8%Si-8%Zn samples are larger than the two previous foam samples. The Al-8%Si-4%Zn sample with a mean pore diameter of about 2.8 mm has the maximum cell size compared to the other fabricated foams, this increase in cell size is due to an increase in the amount of silicon element in the structure of this foam.

In previous work, it was observed that the cell sizes of the foam sample with 8%Si increased with an increase in the silicon element from 4 to 8 wt%,²⁹ these results were also observed in this experiment for Al-8%Si-4%Zn and Al-8%Si-8%Zn samples.

Figure 4 shows the variation of porosity and density of the pure aluminum foam and combination foam specimens. The results obtained from the test of alloy foams show that the density of these foams increases with increasing the amount of zinc element which this due to the effect of zinc on increasing the viscosity of the melt. The density of the pure aluminum foam and aluminum alloy foams with 4%Si-4%Zn, 4%Si-8%Zn, 8%Si-4%Zn, and 8%Si-8%Zn are about 0.6, 1.1, 0.85, 0.68, 0.72 gr/cm³, respectively, where the minimum and maximum values of the foam density belong to the pure aluminum foam and Al-4%Si-4%Zn foam sample, respectively. The experimental results show that the effect of silicon on the surface tension is more dominant than the effect of zinc on the viscosity of the melt and this condition reduces the density of Al-8%Si-4%Zn and Al-8%Si-8%Zn samples compared to the Al-4%Si-4%Zn sample. But the density of the Al-8%Si-8%Zn sample slightly increases due to the increasing amount of zinc element from 4 to 8 wt% in this foam compare to the Al-8%Si-4%Zn sample. The created oxide phases in Al-

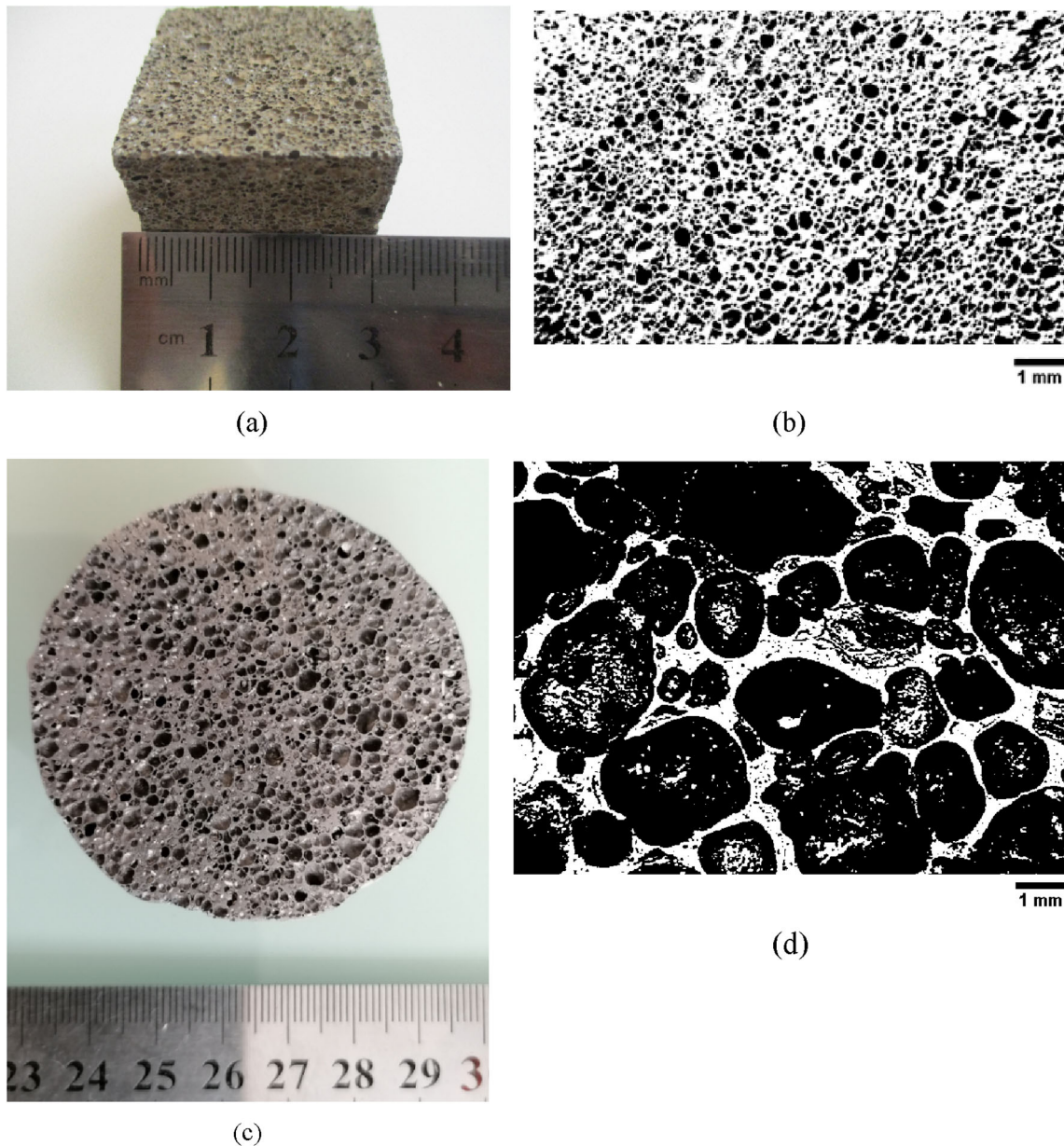


Figure 1. (a) Compressive specimen and (b) binary image J of closed-cell pure Al-foam and also (c) cross section and (d) binary image J of closed-cell Al-8%Si-8%Zn foam.

4%Si-4%Zn foam increase the viscosity of the melt in this sample, high viscosity prevents the growth of bubbles and led to the formation of foams with smaller cell size, thicker cell wall thickness, higher density, and finally, all these factors cause the formation of foam with low porosity. The porosity of pure aluminum foam and aluminum alloy foams with 4%Si-4%Zn, 4%Si-8%Zn, 8%Si-4%Zn, and 8%Si-8%Zn are about 79%, 60%, 68%, 74%, and 73%, respectively, which the maximum and minimum values of porosity belong to the pure aluminum foam and Al-4%Si-4%Zn foam sample, respectively.

The results of x-ray diffraction analysis of two foam specimens containing 4%Si-4%Zn with different stirring times (a) before and (b) after the stirring process have been

shown in Figure 5. The created phases in (a) and (b) samples are Si, SiO₂, CaAl₂Si₂, Ca₃Al₄ZnO₁₀, and Ca₁₄Al₁₀Zn₆O₃₅. As it is clear in Figure 5, the quantity of SiO₂ and Si phases of stirred and non-stirred foam samples are approximately fixed whereas the intensity of these phases in the stirred foam sample has increased (Figure 5(b)). As it is clear in Figure 5(a), in the sample before the stirring process, the Ca₃Al₄ZnO₁₀ phase mostly formed that amount of this phase after stirring is lower and instead, the quantity of Ca₁₄Al₁₀Zn₆O₃₅ phase increases in the stirred foam sample. Also, the brittle phase of CaAl₂Si₂ in the stirred foam sample is more than in the non-stirred foam sample, but the amount and intensity of the Ca₁₄Al₁₀Zn₆O₃₅ and Ca₃Al₄ZnO₁₀ phases increase after the stirring process.

Table 2. Physical Properties of the Fabricated Foams

Matrix	Si, Zn (wt%)	Density (g/cm ³)	Relative density	Porosity (%)
Al 99.8%	0%Si- 0%Zn	0.56	0.2	79.009
Al 99.8%	4%Si- 4%Zn	1.07	0.39	60.21
Al 99.8%	4%Si- 8%Zn	0.85	0.31	68.44
Al 99.8%	8%Si- 4%Zn	0.67	0.25	74.83
Al 99.8%	8%Si- 8%Zn	0.71	0.26	73.41

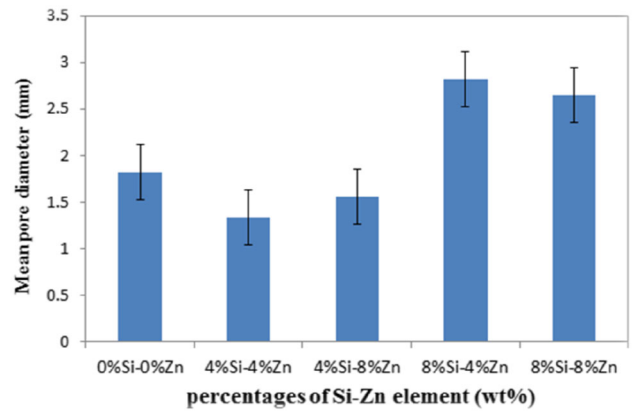


Figure 3. Mean pore diameter of the foams with different silicon and zinc contents.

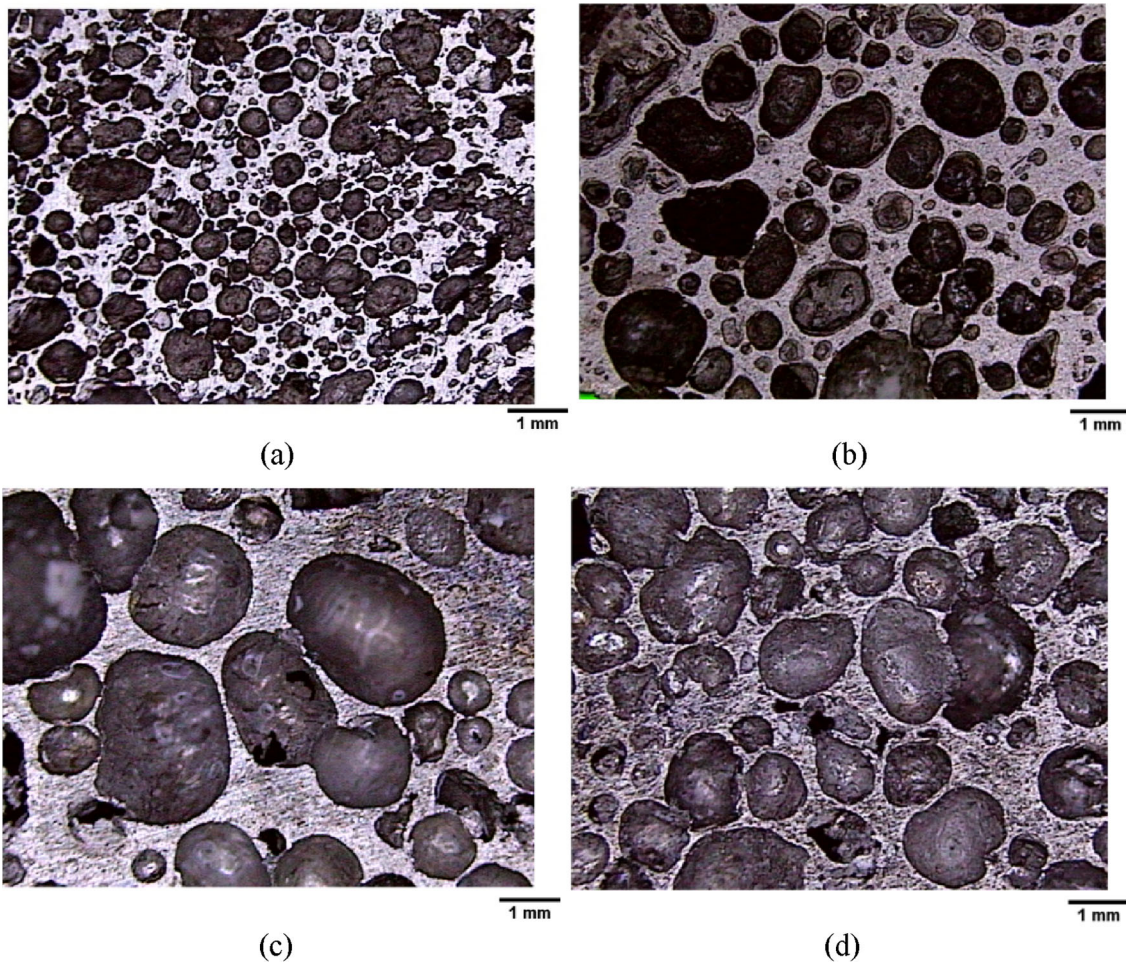


Figure 2. Optical-macrographs of (a) Al-4%Si-4%Zn, (b) Al-4%Si-8%Zn, (c) Al-8%Si-4%Zn, and (d) Al-8%Si-8%Zn samples.

The microstructure of Al-4%Si-4%Zn samples (a) before and (b) after the stirring process has been shown in Figure 6. As shown in Figure 6, the foam has a matrix of Al (1) and the oxide phases (2) that are scattered between the

eutectic structure, and the amount of these phases by the stirring process was increased. Also, the needle-shaped structures (3) in the structure of these samples were formed.

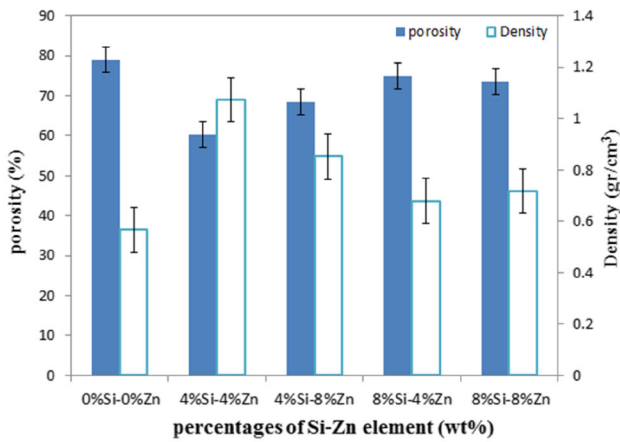


Figure 4. Variation of density and porosity of foams with different percentages of Si and Zn contents.

According to the experimental results of previous work for samples with 4%Si and 4%Zn^{28,29} and comparing them with the results obtained in this experiment for the Al-4%Si-4%Zn sample, it was found that the compounds and phases by the addition of silicon and zinc created into the structure of these foams, causes increase the melt viscosity that amount of these phases with the stirring the melt was increased. Since the intermetallic phases were formed

immediately after the dissolution of calcium into the melt and the viscosity of the melt has not very increased, it seems that the oxide phases of $\text{Ca}_3\text{Al}_4\text{ZnO}_{10}$ and $\text{Ca}_{14}\text{Al}_{10}\text{Zn}_6\text{O}_{35}$ which were formed during the stirring of the Al-4%Si-4%Zn sample, and increased the melt viscosity and finally, all of these factors have led to the formation of foam with a small cell structure in this sample.

Compressive and Energy Absorption Results

The engineering stress–strain curves of combination foams are shown in Figure 7. Also, for comparison and understanding of the changes in the stress–strain curves of combination foams, the stress–strain curve of aluminum foam has been shown for comparison. As shown in the curves, the Al-4%Si-4%Zn and Al-4%Si-8%Zn samples have good properties compared to the other samples. Generally, the energy absorption and strength of the Al-8%Si-4%Zn and Al-8%Si-8%Zn samples were decreased compared to the Al-4%Si-4%Zn and Al-4%Si-8%Zn foams samples. Indeed, due to the presence of silicon content in the structure and the formation of brittle structures such as CaAl_2Si_2 in the structure of Al-8%Si-4%Zn and Al-8%Si-8%Zn samples, the compressive strength of these samples

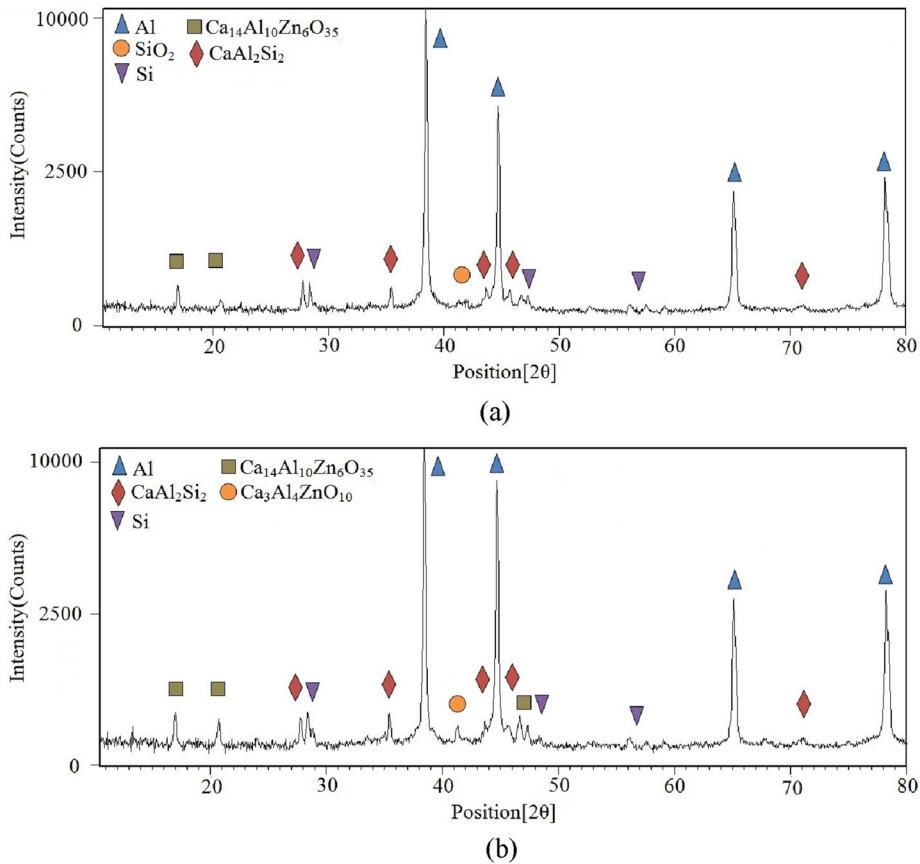


Figure 5. X-ray diffraction analysis of Al-4%Si-4%Zn foam (a) before and (b) after the stirring process.

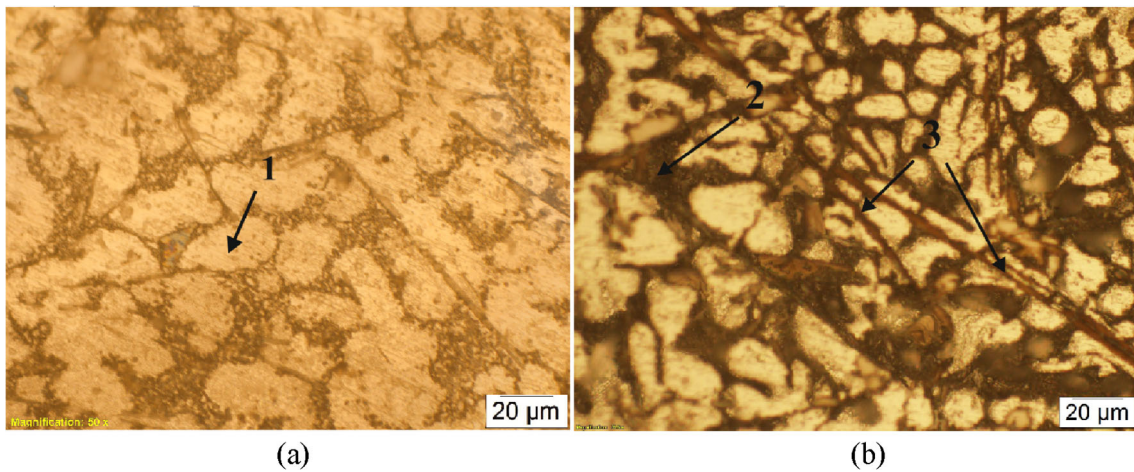


Figure 6. Microstructure of Al-4%Si-4%Zn samples (a) before and (b) after the stirring process.

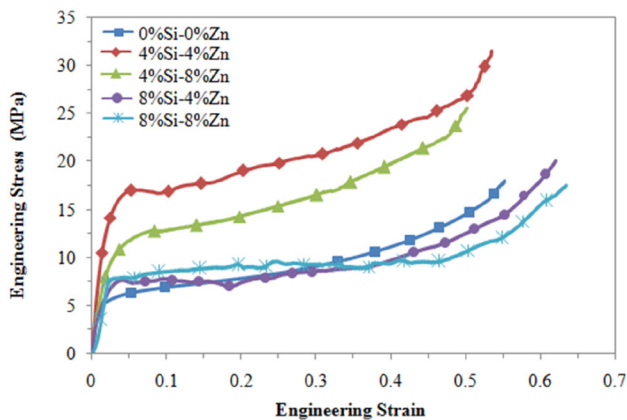


Figure 7. Engineering stress–strain curves of combination foams.

is reduced. The amount of brittle formed phase of CaAl_2Si_2 in Figure 5(b) is low and decreases the amount of this phase increases the strength of the Al-4%Si-4%Zn and Al-4%Si-8%Zn samples, but with an increase in the Si content in Al-8%Si-4%Zn and Al-8%Si-8%Zn samples, the brittle phase CaAl_2Si_2 more creates which makes the structure of these samples brittle and reduces the strength of these samples compared to Al-4%Si-4%Zn and Al-4%Si-8%Zn. From the stress–strain curves in Figure 7, it can be seen that the stress–strain curves of the Al-4% Si-4% Zn and Al-4% Si-8% Zn samples are uniform and there are no fractures in them. However, in Al-8% Si-4% Zn and Al-8% Si-8% Zn samples, the stress–strain curves are dendritic and failure was observed in the structure of these samples. All of these factors are due to the increase in the effect of silicon content on the structure and the formation of more brittle compounds in Al-8%Si-4%Zn and Al-8%Si-8%Zn samples compare to the Al-4%Si-4%Zn and Al-4%Si-8%Zn samples.

As previously mentioned, the yield strength of pure aluminum foam is 4.8 MPa and this amount for Al-4%Si-4%Zn and Al-4%Si-8%Zn alloy foams are measured at

13.6 and 9.4 MPa, respectively, however, the yield strength values of Al-8%Si-4%Zn and Al-8%Si-8%Zn foams are 7 and 8.8MPa, respectively, which increased in comparison with the pure aluminum foam but have decreased compared to Al-4%Si-4%Zn and Al-4%Si-8%Zn foams. Figure 8 shows the yield strength and densification strain for combination foams.

The densification strain of the Al-4%Si-4%Zn sample increases compare to pure aluminum foam, but this amount reduces for the Al-4%Si-8%Zn sample; whereas the densification strain for Al-8%Si-4%Zn and Al-8%Si-8%Zn samples increased compared to all of the samples. The densification strain values of pure aluminum foam and Al-4%Si-4%Zn, Al-4%Si-8%Zn, Al-8%Si-4%Zn and Al-8%Si-8%Zn combination samples are about 0.46, 0.5, 0.45, 0.56 and 0.58, respectively. The energy absorption capacity curves of pure aluminum foam and combination foams are shown in Figure 9.

The energy absorption capacity of pure aluminum foam is 7 MJ/m^3 in the strain rate of 0.5, while these amounts for Al-4%Si-4%Zn, Al-4%Si-8%Zn, Al-8%Si-4%Zn, and Al-

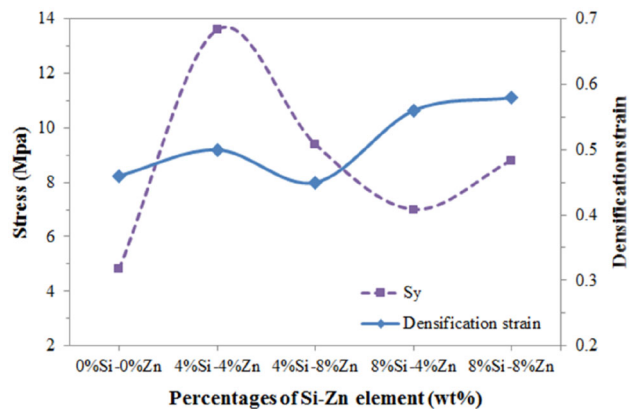


Figure 8. Variation of the yield strength and densification strain of combination foams.

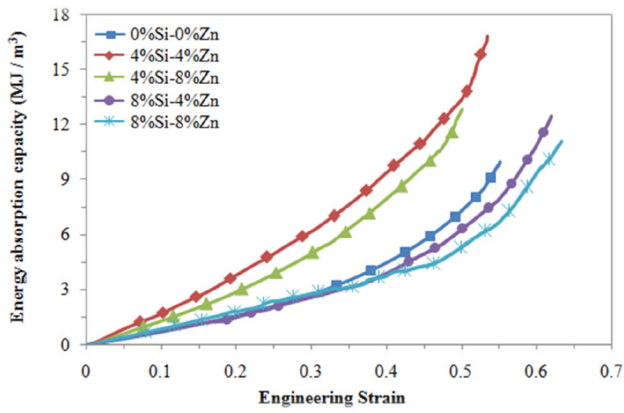


Figure 9. Energy absorption curves of combination foams.

8%Si-8%Zn foam samples are about 13.7, 12.5, 6.2, and 4.8MPa, respectively. These indicate that the energy absorption capacity of Al-4%Si-4%Zn and Al-4%Si-8%Zn foams increase in comparison with pure aluminum foam, but this value decreases for Al-8%Si-4%Zn and Al-8%Si-8%Zn samples. In general, it was found that compounds and phases created in alloy foams change the compressive behavior of these foams. The optical metallography of Al-8%Si-4%Zn and Al-8%Si-8%Zn samples are shown in Figure 10.

The microstructure of Al-8%Si-4%Zn and Al-8%Si-8%Zn samples with higher magnification are shown in Figure 11. As clear from these figures the oxide phases were separated by needle structures (1-region) which created structure except in the Al-4%Si-4%Zn sample was not observed in the other specimens. Also, precipitates identified as silicon

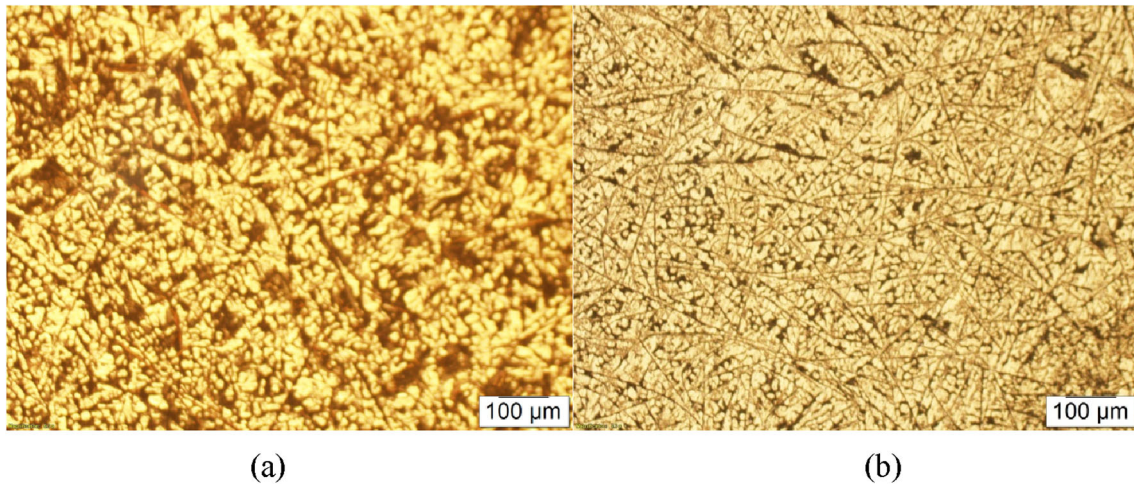


Figure 10. Microstructure of (a) Al-8%Si-4%Zn and (b) Al-8%Si-8%Zn alloy foam samples.

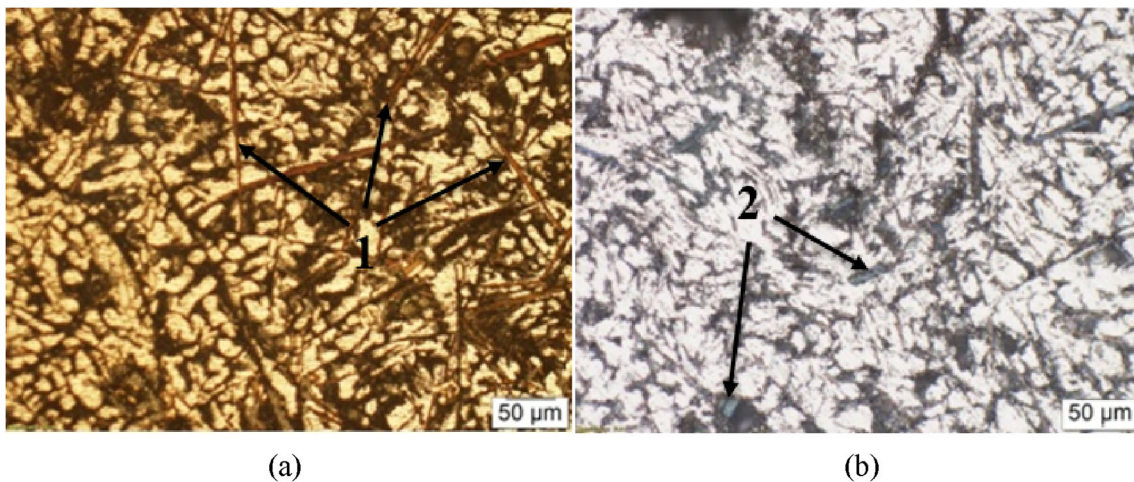
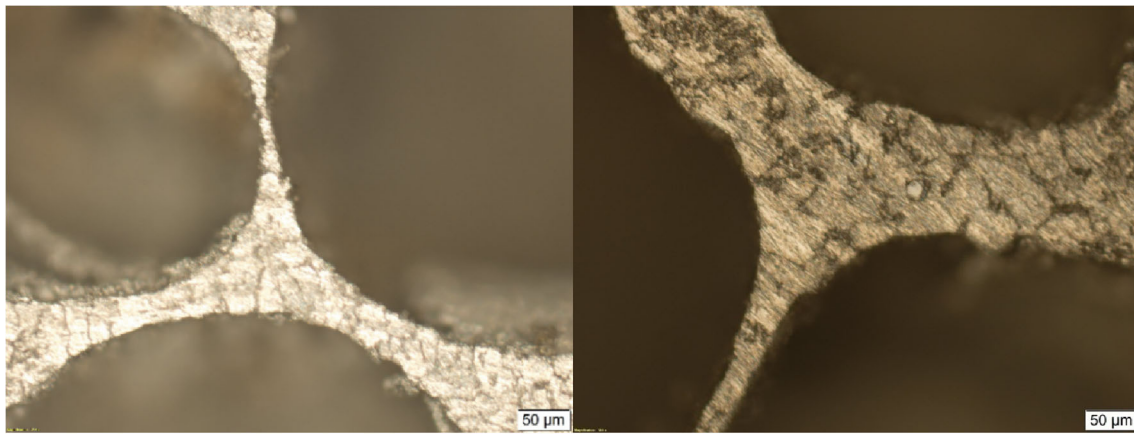


Figure 11. Precipitate and oxide phases in the microstructure of (a) Al-8%Si-4%Zn and (b) Al-8%Si-8%Zn alloy foam samples.



(a) (b)

Figure 12. Optical microscopic images of the cell wall thickness of (a) Al-4%Si-4%Zn and (b) Al-8%Si-8%Zn foams.

particles (2-region) were formed in the structure of the Al-8%Si-8%Zn sample and they accumulated in certain areas of this foam.

As seen in Figure 11, the presence of coarse and needle-shaped structures in some regions, as well as the presence of silicon particles can be early seen as phases in the structure of Al-8%Si-4%Zn and Al-8%Si-8%Zn alloy foams. Earlier it was said that silicon reduces the surface tension of the melt which reduces cell wall thickness in foam and increases the size of cells.^{35,36} As shown in Figure 12, reducing in the surface tension of Al-8%Si-4%Zn and Al-8%Si-8%Zn samples cause an increase in the cell size and a decrease in the cell wall thickness with an increase in the amount of silicon of these samples which also these cases were observed on the effect of Si on the structure of Al-based foams for the foam sample with 8%Si in the previous study. It has been observed that most alloys containing silicon have a minimum cell wall thickness

between 50 to 80μm.³⁷ The average cell wall thickness of pure aluminum foam is 93.5μm, while these amounts for Al-4%Si-4%Zn, Al-4%Si-8%Zn, Al-8%Si-4%Zn, and Al-8%Si-8%Zn samples are about 81.88, 74.98, 41.3, and 43.2μm, respectively. The cell wall thickness of samples Al-4%Si-4%Zn and Al-8%Si-8%Zn are shown in Figure 12.

The variation of density and absorbed energy per unit volume at the strain of 0.5 for pure aluminum foam and aluminum alloy foams are shown in Figure 13. The highest values of density and energy absorbed per unit volume belong to the Al-4%Si-4%Zn sample and their lowest values belong to the Al-4%Si-8%Zn sample whereas these values are nearly the same for Al-8%Si-4%Zn and Al-8%Si-8%Zn samples.

According to the results, it was found that the differences in the microstructure, intermetallic compounds, and phases created in the alloy foams affected the characterization of fabricated foams. The intermetallic compounds created in the structure of the foam are different from the structure of the base material which these compounds were more observed in the Al-8%Si-4%Zn and Al-8%Si-8%Zn samples, whereas these volumes of compounds were not observed in Al-4%Si-4%Zn and Al-4%Si-8%Zn alloy foams. However, small particles that are widely distributed in the foam structure were found in the structure. The Al-4%Si-4%Zn and Al-4%Si-8%Zn alloy foams have a fine morphology compared to the other samples, which can be attributed to the uniform distribution of intermetallic compounds created in the cell wall structure of these samples. These items can be seen in Figures 14 and 15.

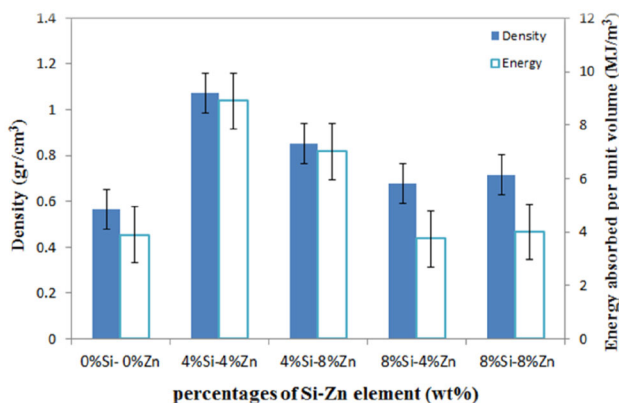
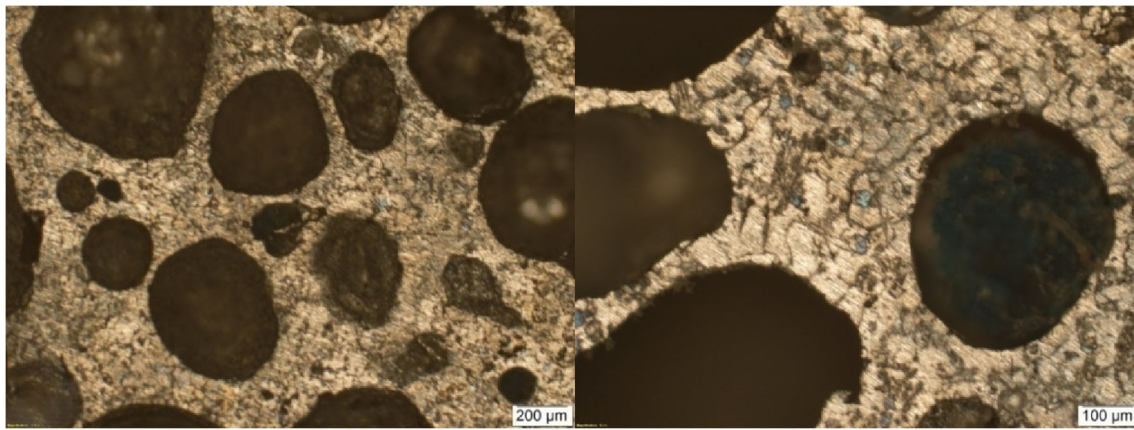


Figure 13. The variation tendency of density and absorbed energy per unit volume in the strain of 0.5.



(a)

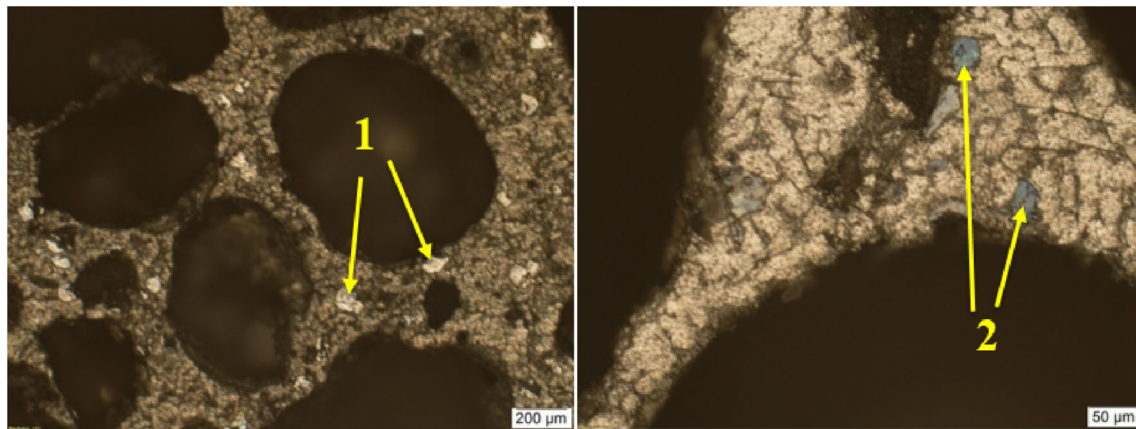
(b)

Figure 14. The microstructures of (a) Al-4%Si-4%Zn and (b) Al-4%Si-8%Zn samples.

The compression behavior of the alloy foams changed due to the effect of silicon content on the structure of these foams. The formation of intermetallic compounds based on calcium is brittle, as the addition of calcium leads to the formation of a coarse and brittle structure from Al-Si compounds similar to CaAl_2Si_2 in the cell wall structure of these foams.^{29,38} The x-ray analysis shows that the brittle phase of CaAl_2Si_2 has been formed in the structure of Al-silicon foams as this phase exists in the Al-8%Si-4%Zn and Al-8%Si-8%Zn samples. As can be seen in Figures 11 and 15, the existence of this phase as well as the formation of the needle structures (region of (1) in Figure 11(a)), silicon particles (region of (2) in Figure 11(b)), and intermetallic

compounds (region of (1) in Figure 15) formed in the foam structure (Figure 15) increase the brittle fracture of foams and reduce the strength and energy absorption capacity of these foams. Also, similar results about the addition of manganese to the structure of aluminum foam were observed by other researchers.³⁹ The microstructures of Al-8%Si-4%Zn and Al-8%Si-8%Zn samples are shown in Figure 15(a) and (b), respectively.

The energy absorption capacities of Al-8%Si-4%Zn and Al-8%Si-8%Zn foams samples are lower than their Al-4%Si-4%Zn and Al-4%Si-8%Zn foams samples decreased this is probably due to larger cell size and the formation of



(a)

(b)

Figure 15. Distribution of particles and intermetallic compounds created in the structure of (a) Al-8%Si-4%Zn and (b) Al-8%Si-8%Zn samples.

more brittle compounds in the cell walls of these samples, which causes the cell wall to buckle under pressure and break easily. For most alloy foams, the increase in alloying elements increases the ability to absorb energy, which is reasonable because more metal intermetallic compounds are formed.³⁹ However, this behavior was not observed in foams containing 8%Si-4%Zn and 8%Si-8%Zn because increasing the content of silicon leads to a decrease in the strength and energy absorption in these foams.

Conclusions

In the present experimental study, the effects of different percentages of silicon and zinc contents were investigated on the morphology and mechanical properties of closed-cell aluminum foam. The effects of alloying elements were studied on the compressive property and energy absorption of aluminum-based foams. Also, the effect of created phases and intermetallic compounds which is due to the addition of these elements in the structure of foams were investigated that results are as follows:

- The Al-4%Si-4%Zn foam sample has a smaller cell size and a thicker cell wall, and the high volume fraction of oxide compounds and phases created in the foam structure increases the viscosity and reduces the cell size of these foams.
- The Al-4%Si-4%Zn and Al-4%Si-8%Zn alloy foams have good properties in terms of strength and energy absorption compared to the other fabricated foams due to the uniform distribution of intermetallic compounds in the cell wall of these foams.
- Adding silicon to the melt, in addition to reducing the surface tension, increases the cell size, leads to a reduction of the cell wall thickness, and causes the formation of more brittle structures and intermetallic compounds were formed in Al-8%Si-4%Zn and Al-8%Si-8%Zn samples.
- The result shows that the existence of the brittle phase of CaAl_2Si_2 in the structure of the Al-8%Si-4%Zn and Al-8%Si-8%Zn samples and also the formation of needle-shaped structures and intermetallic compounds and accumulation of these compounds in the cellular structure and cell wall reduce the strength and increase the plateau region of these foams more than the other foams samples.

REFERENCES

1. K.C. Chan, S. Chan, Effect of cell morphology and heat treatment on compressive properties of aluminum foams. *Mater. Manuf. Process.* **19**(3), 407–422 (2004)
2. M. Gauthier et al., Production of metallic foams having open porosity using a powder metallurgy approach. *Mater. Manuf. Process.* **19**(5), 793–811 (2004)
3. M. Avalle et al., AlSi7 metallic foams—aspects of material modelling for crash analysis. *Int. J. Crashworthiness* **14**(3), 269–285 (2009)
4. M.F. Ashby, T. Lu, Metal foams: a survey. *Sci. China, Ser. B: Chem.* **46**(6), 521–532 (2003)
5. M.F. Ashby et al., *Metal Foams: A Design Guide* (Elsevier, Amsterdam, 2000)
6. Y. Cheng et al., Compressive properties and energy absorption of aluminum foams with a wide range of relative densities. *J. Mater. Eng. Perform.* **27**(8), 4016–4024 (2018)
7. K. Grilec, G. Marić, S. Jakovljević, A study on energy absorption of aluminium foam. *BHM Berg-und Hüttenmännische Monatshefte* **155**(5), 231–234 (2010)
8. A. Bisht, V.K. Patel, B. Gangil, Future of metal foam materials in automotive industry, in *Automotive Tribology*. (Springer, Berlin, 2019), pp. 51–63
9. F. García-Moreno, Commercial applications of metal foams: their properties and production. *Materials* **9**(2), 85 (2016)
10. N. Gupta, R. Maharsia, Enhancement of energy absorption in syntactic foams by nanoclay incorporation for sandwich core applications. *Appl. Compos. Mater.* **12**(3), 247–261 (2005)
11. X. Song et al., Crashworthiness optimization of foam-filled tapered thin-walled structure using multiple surrogate models. *Struct. Multidiscip. Optim.* **47**(2), 221–231 (2013)
12. F. Binesh, J. Zamani, M. Ghiasvand, Ordered structure composite metal foams produced by casting. *Inter Metalcast.* **12**(1), 89–96 (2018). <https://doi.org/10.1007/s40962-017-0143-x>
13. A.H. Astaraie, H. Shahverdi, S. Elahi, Compressive behavior of Zn–22Al closed-cell foams under uniaxial quasi-static loading. *Trans. Nonferrous Metals Soc. China* **25**(1), 162–169 (2015)
14. A. Manonukul et al., Effects of replacing metal powder with powder space holder on metal foam produced by metal injection moulding. *J. Mater. Process. Technol.* **201**(3), 529–535 (2010)
15. B. Wang, E. Zhang, On the compressive behavior of sintered porous coppers with low-to-medium porosities—Part II: preparation and microstructure. *Int. J. Mech. Sci.* **50**(3), 550–558 (2008)
16. S. Yu et al., Compressive behavior and damping property of ZA22/SiCp composite foams. *Mater. Sci. Eng., A* **457**(1–2), 325–328 (2007)
17. J. Banhart, Metallic foams: challenges and opportunities. *Eurofoam* **2000**, 13–20 (2000)
18. X. Xia et al., Effect of homogenizing heat treatment on the compressive properties of closed-cell Mg alloy foams. *Mater. Des.* **49**, 19–24 (2013)

19. V. Jeenager, V. Pancholi, B. Daniel, The effect of aging on energy absorption capability of closed cell aluminum foam. In *Advanced Materials Research*. 2012. Trans Tech Publ
20. D.-H. Yang et al., Compression properties of cellular AlCu5Mn alloy foams with wide range of porosity. *J. Mater. Sci.* **44**(20), 5552–5556 (2009)
21. V. Davydov et al., Scientific principles of making an alloying addition of scandium to aluminium alloys. *Mater. Sci. Eng., A* **280**(1), 30–36 (2000)
22. Y. Harada, D. Dunand, Microstructure of Al3Sc with ternary rare-earth additions. *Intermetallics* **17**(1–2), 17–24 (2009)
23. Y. Ye, P. Li, L. He, Valence electron structure analysis of morphologies of Al3Ti and Al3Sc in aluminum alloys. *Intermetallics* **18**(2), 292–297 (2010)
24. X. Xia et al., The compressive properties of closed-cell aluminum foams with different Mn additions. *Mater. Des.* **51**, 797–802 (2013)
25. W.-M. Zhao et al., Compressive characteristics of closed-cell aluminum foams with different percentages of Er element. *China Foundry* **13**(1), 36–41 (2016)
26. T. Savaşkan, A. Aydıner, Effects of silicon content on the mechanical and tribological properties of monotelectoid-based zinc–aluminium–silicon alloys. *Wear* **257**(3–4), 377–388 (2004)
27. S.-H. Park et al., Thermophysical properties of Al and Mg alloys for metal foam fabrication. *Colloids Surf. A* **263**(1–3), 280–283 (2005)
28. M.R. Farahani, H.R. Rezaei Ashtiani, S.H. Elahi, Effect of zinc content on the mechanical properties of closed-cell aluminum foams. *Inter Metalcast.* **16**, 713–722 (2022). <https://doi.org/10.1007/s40962-021-00635-2>
29. M.R. Farahani, H.R.R. Ashtiani, S. Elahi, Effect of silicon content on mechanical properties and progressive collapse behavior of closed-cell aluminum foams. *Trans. Indian Inst. Metals* **74**, 3145–3154 (2021)
30. L. Huang et al., Effects of scandium additions on mechanical properties of cellular Al-based foams. *Intermetallics* **28**, 71–76 (2012)
31. Standard, I., ISO 13314: 2011 (E)(2011) Mechanical testing of metals—ductility testing—compression test for porous and cellular metals. Ref Number ISO. **13314**(13314): p. 1–7
32. X. Xia et al., Compressive properties of closed-cell aluminum foams with different contents of ceramic microspheres. *Mater. Des. (1980–2015)* **56**, 353–358 (2014)
33. W.H. Yang et al. Mechanical Properties and Energy Absorption Capability of Closed-Cell Al Alloy Foam. In *Advanced Materials Research*. 2012. Trans Tech Publ
34. M. Aboaraia, R. Sharkawi, M. Doheim, Production of aluminium foam and the effect of calcium carbonate as a foaming agent. *J. Eng. Sci. Assiut Univ.* **39**(2), 441–451 (2011)
35. J. Banhart, Metal foams: production and stability. *Adv. Eng. Mater.* **8**(9), 781–794 (2006)
36. B.Y. Hur, S.H. Park, A. Hiroshi. Viscosity and surface tension of Al and effects of additional element. In *Materials Science Forum*. 2003. Trans Tech Publ
37. H. Stanzick et al., Process control in aluminum foam production using real-time X-ray radiography. *Adv. Eng. Mater.* **4**(10), 814–823 (2002)
38. A. Byakova et al., Improvements in stabilisation and cellular structure of Al based foams with novel carbonate foaming agent. *High Temp. Mater. Process. (London)* **26**(4), 239–246 (2007)
39. L.A. Perales, *On the Stabilization of Aluminum Foams by Tin Additions and in Situ Intermetallic Formation* (McGill University Libraries, Montreal, 2015)

Publisher's Note Springer Nature remains neutral with regard to jurisdictional claims in published maps and institutional affiliations.